SOME PHYSICAL MODELS OF THE REACTION-DIFFUSION EQUATION AND COUPLED MAP LATTICES

YAKOV PESIN AND ALEX YURCHENKO

ABSTRACT. We review a number of models which appear in physics, biology, chemistry, etc. and which are described by the reaction-diffusion equation. By discretazing this equation we obtain the corresponding coupled map lattice (CML) system. We classify these CMLs by the type of the dynamics of the local map. We observe several different types of behavior, namely, Morse-Smale type systems, systems with attractors, and systems with Smale horseshoes.

1. INTRODUCTION.

In this paper we review a number of important models in physics, biology, and chemistry which are described by the non-linear reaction-diffusion equation

$$u_t = h(u) + \mathcal{A}\kappa\triangle u,$$

where $x \in \mathbb{R}^p$, $u = u(x, t)$ is a function with values in $\mathbb{R}^d$, $\mathcal{A}$ a matrix, and κ a parameter. This equation represents extended systems of unbounded equilibrium media with energy pumping and the function u is a characteristic of the medium (for example, its density, or distribution of temperature). In Section 2 we discribe the models while in Section 3 we classify them according to their type.

We are interested in the dynamics of the corresponding coupled map lattice (CML) that is a discrete versions of this equation, i.e.,

$$u_{\bar{j}}(n + 1) = f(u_{\bar{j}}(n)) + \varepsilon g_{\bar{j}}(\{u_{\bar{i}}(n)\}_{|\bar{i}-\bar{j}|\leq s}),$$

where $n \in \mathbb{Z}$ is the discrete time coordinate and $\bar{j} = (j_k)$, $k = 1, ..., p$ the discrete space coordinate. We assume that $f : \mathbb{R}^d \to \mathbb{R}^d$ and

1

$g_{\bar{j}} : (\mathbb{R}^d)^{(2s+1)^p} \to \mathbb{R}^d$ are smooth maps; f is called the *local map* and it acts in the *local phase space* (which is either $\mathbb{R}^d$ or its compactification S^d); g is the *interaction of finite size s*. We also assume that ε is a sufficiently small parameter (see Section 4).

One can think of a CML as an infinite collection of copies of the *local dynamical system* $(f, \mathbb{R}^d)$ associated with each point in the lattice $\mathbb{Z}^d$. When $\varepsilon = 0$ the local dynamics at different points of the lattice do not depend on each other. However, for small ε the dynamics at a given point of the lattice "feels" the local dynamics at neighboring points (within the lattice cube of size s). In the cases, where the local dynamics displys strong hyperbolic behavior, the dynamics of CML is completely determined by the local dynamics (provided ε is sufficiently small). See [1, 2]. The goal of this paper is to analize the local dynamics in some "physicall interesting" cases.

When a CML is obtained from a partial differential equation (PDE) there are two ways to ensure that ε is small: 1) to require that the corresponding parameter of the PDE (usually the diffusion coefficient) is small and 2) to select small discretization steps appropriately.

In what follows, we will fix the discretization step and will vary "the physical parameters" of the system. It turns out that CML's obtained in this way can often be viewed as initial phenomenological models of the underlying processes and in many cases may be better adopted to them.

In the Sections 5 and 6 we classify CML under consideration by the type of the dynamics of their local maps. It turns out that when the local map is one-dimensional the dynamics is of Morse-Smale type in some range of parameters. When the local map is the two-dimensional the dynamics is much richer: by varying parameters of the system one can observe a Morse-Smale type behavior, existence of Smale horseshoes, or "strange" attractors. We illustrate this by study of the dynamics of the local map of the FitzHugh-Nagumo equation (see Section 6).

2. Models From Science.

Here we present several examples from different branches of science that are described by evolution PDE's.

2.1. **Fisher model in population genetics** [26]**.** The model describes a population of diploid individuals (i.e., the ones that carry two genes) distributed in a flat two dimensional habitat. Assuming that a gene occurs in two forms a and A, called *alleles*, one can divide the population into three genotypes aa, aA, and AA. Let $u_i = u_i(t, x)$, $i \in \{1, 2, 3\}$, be the population densities of aa, aA, and AA respectively. Assume that members of the population mate at random, with a birth rate r, and diffuse through the habitat with a diffusion constant D. Assume further that death rates depend only on the genotypes and denote them by τ_i, $i = 1, 2, 3$. Thus, $u_i(x, t)$ changes due to diffusion, mating, and death.

It is shown in [3] that if $|\tau_1 - \tau_2| + |\tau_3 - \tau_2| \ll 1$ and $r \gg 1$ then the function

$$u = \frac{u_3 + \frac{1}{2} u_2}{u_1 + u_2 + u_3}$$

satisfies the following PDE

(2.1.1) $$u_t = -\sigma u (u - \theta)(u - 1) + D \triangle u,$$

where $\sigma = \sigma(\tau_1, \tau_2, \tau_3) > 0$ and $\theta = \theta(\tau_1, \tau_2, \tau_3)$, $0 < \theta < 1$ are parameters.

2.2. **Kolmogorov-Petrovskii-Piskunov (KPP) planar model of advance of advantageous genes** [16]**.** Consider a two dimensional area populated by individuals of a given species. Assume that the population has a dominant allele A, that is, the chance of survival of individuals with this allele is larger than individuals that do not posses this gene.

In the case when the dominant allele is distributed over the area with a constant concentration p the change of p per one generation can be obtained by the formula (see [9])

$$\delta p = \alpha p (1 - p)^2 + O(\alpha^2),$$

where $\alpha + 1$ is the ratio of the probability that an individual with dominant allele A survives to the corresponding probability for an individual without the allele A.

We now consider the case when the concentration p changes in time and space due to the selection in favor of the dominant allele A and to random motions of individuals. Assume finally that the root-mean-square path ρ of an individual during one generation is sufficiently

small. One can show that the change in the concentration per generation can be found by the formula

(2.2.2)
$$\delta p(x,y) = \int_{\mathbb{R}} \int_{\mathbb{R}} p(\zeta,\xi)\frac{f(r)}{2\pi r}d\zeta d\xi - p(x,y) + \alpha p(x,y)(1-p(x,y))^2,$$

where $f(r)dr$ is the probability that an individual passes a distance lying between r and $r + dr$ with $r = \sqrt{(x-\zeta)^2 + (y-\xi)^2}$. Assuming that p is differentiable with respect to the coordinates x, y, and time t and that $\alpha \ll 1$ we can expand (2.2.2) into a Taylor series to obtain

(2.2.3)
$$p_t = \alpha p(1-p)^2 + \frac{\rho^2}{4}\triangle p.$$

2.3. Fisher linear model of advance of advantageous genes [10].

Consider a population of a given species distributed uniformly along a linear habitat, such as a shore line. Assume that the size of the habitat is large compare with the distances separating the sites of offsprings from those of their parents. Assume further that at some point of the habitat an advantageous mutation (that is a mutation that is somehow advantageous to the survival of a member of the population) occurs. This mutation diffuses, first, into the neighborhood of the occurrence of mutation and then into the surrounding population. This process is due to selection in favor of the advantageous mutation and to random motions of individuals.

Let $p = p(x,t)$ be the concentration of the members of the population with the mutant gene and $q = q(x,t)$ the concentration of the members of the population whose offsprings have the mutant gene (x is a position in the habitat). One can assume that $q = 1 - p$. Denote by α the intensity of selection in favor of the mutant gene, which we assume to be independent of p. For sufficiently small α the concentration p varies continuously with time from generation to generation. Suppose that the rate per generation at which members of the population with the mutant gene diffuse into the whole population is given by $-\kappa\frac{\partial p}{\partial x}$, where $\kappa > 0$ is a diffusion constant (assumed to be independent of x and p). This corresponds to the *ordinary law of diffusion* that is diffusion is proportional to the gradient of the concentration. Under all these assumptions one can show that the concentration of the mutant gene satisfies:

(2.3.4)
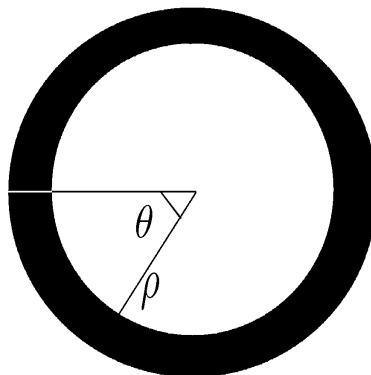$$\frac{\partial p}{\partial t} = \alpha p(1-p) + \kappa\frac{\partial^2 p}{\partial x^2}.$$

FIGURE 1. Idealized Embryo.

2.4. **Turing's continuous model of morphogenesis** [29]. The morphogenesis is an embryological development of the structure of an organism or some part of an organism. Turing suggested a model of an idealized embryo which contains two characteristic chemical substances $\mathcal{X}$ and $\mathcal{Y}$ called *morphogens*. These substances react with each other in each cell and diffuse between neighboring cells with diffusibility coefficients μ and ν respectively. Consider an idealized embryo which is realized as an annulus of the inner radius ρ of tissue (see Figure 1). Denote by X and Y concentrations of the corresponding chemicals. Let $f(X, Y)$ and $g(X, Y)$ be the rates at which concentrations X and Y respectively change due to the chemical interaction. The reaction rates are assumed to obey the *law of mass action* that states that the rate at which a reaction takes place is proportional to the concentrations of the reacting substances. We assume that diffusion obeys the *ordinary law of diffusion*. In this case this means that each morphogen moves from the region of greater to the region of less concentration at a rate proportional to the gradient of the concentration. Then the governing equations are

(2.4.5)
$$X_t = f(X, Y) + \frac{\mu}{\rho^2} X_{\theta\theta},$$
$$Y_t = g(X, Y) + \frac{\nu}{\rho^2} Y_{\theta\theta},$$

where θ is the angle between the radius to the point and a fixed reference radius (see Figure 1). Turing used the following formulas for the rate functions

$$f(X, Y) = -aX^2 - bXY + d,$$
$$g(X, Y) = aX^2 + bXY - cY + e,$$

where $a, b, c, d, e \in \mathbb{R}^+$ are parameters of the reaction.

2.5. Maginu model of morphogenesis [17].

This model is a simplification of the above Turing model. A single cell is viewed as an electrical circuit similar to the one used by Nagumo (see Section 2.8 below and Figure 3). Arranging these cells on a ring by coupling neighboring ones, Maginu produced a system of reaction-diffusion PDE's

$$(2.5.6) \qquad \begin{aligned} X_t &= -aX(X-1)(X+1) - Y + \kappa_1 X_{\theta\theta}, \\ Y_t &= \varepsilon(X - \gamma Y) + \kappa_2 Y_{\theta\theta}, \end{aligned}$$

where X and Y are concentrations of two types of morphogens, a, κ_1, κ_2, ε, and γ are positive parameters. Note that the nonlinear term in (2.5.6) is simpler than the nonlinear term in (2.4.5).

2.6. The FitzHugh's model of the propagation of voltage impulse through a nerve axon.

In [14], Hodgkin and Huxley proposed a model to describe the ionic and electrical events occurring during the transmission of an impulse through the surface membrane and the propagation of voltage impulse through a nerve axon. One can think of the axon as a long cylindrical cable with a conducting core and a partially insulating shell submerged into a large volume of conducting fluid - an ionic solution of either sodium or chloride.

The total density I of the current through the membrane is

$$(2.6.7) \qquad I = C_M \frac{dV}{dt} + I_i,$$

where V is the displacement of the membrane potential from its resting value; C_M the membrane capacity per unit area (assumed to be constant); and $I_i = I_{Na}(V) + I_K(V) + I_l(V)$ the ionic current density which consists of three components carried by: sodium ions (I_{Na}), potassium ions (I_K), and other ions (I_l). The expression for ionic currents densities I_{Na}, I_K, and I_l were obtained experimentally.

The current density through the membrane can be computed by the formula

$$(2.6.8) \qquad I = \frac{\rho}{2R} \frac{\partial^2 V}{\partial x^2},$$

where x is the distance along the fibre, R the specific resistance of the axoplasm, and ρ the radius of the fibre. Combining (2.6.7) and (2.6.8) we obtain that

$$\frac{\rho}{2R} \frac{\partial^2 V}{\partial x^2} = C_M \frac{dV}{dt} + I_i(V).$$

The Hodgkin-Huxley model consists of four differential equations and is yet to difficult for rigorous mathematical analysis. For the detailed discussion of Hodgkin-Huxley model see [6].

In [11], R. FitzHugh suggested a model for the propagation of voltage impulse through a nerve axon which is substantially simpler than the Hodgkin-Huxley model and therefore, is often used in applications.

R. FitzHugh treated the nerve cell as a non-linear electric oscillator

$$\ddot{v} + (v^2 - 1)\dot{v} + cv = 0,$$

where v is a dimensionless variable corresponding to the membrane potential V and $c > 0$ a constant. Setting

$$w = -\dot{v} + v - \frac{v^3}{3}$$

reduces the above second order differential equation to the well-known Bonhoeffer-van der Pol (BVP) system of differential equations of the first order

$$\dot{v} = v - \frac{v^3}{3} - w,$$
$$\dot{w} = cv.$$

The variable w is called the *recovery variable*. R. FitzHugh further modified this system as follows

$$(2.6.9) \qquad \begin{aligned} \dot{v} &= v - \frac{v^3}{3} - w + i, \\ \dot{w} &= c(v + a - bw), \end{aligned}$$
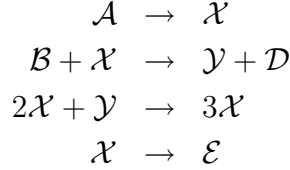
where a and b are positive constants and i a dimensionless variable corresponding to the total membrane current density. Combining (2.6.9) and (2.6.8) we obtain the system of two differential equations:

$$(2.6.10) \qquad \begin{aligned} v_t &= v - \frac{v^3}{3} - w + \kappa v_{xx} \\ w_t &= c(v + a - bw). \end{aligned}$$

where κ is proportional to $\frac{\rho}{2R}$. If no recovery is present (i.e., $w = 0$) we obtain the one-dimensional FitzHugh model (see [12]):

$$(2.6.11) \qquad v_t = v - \frac{v^3}{3} + \kappa v_{xx}.$$

2.7. Brusselator model for the Belousov-Zhabotinsky reaction (BZR) [8].

The BZR is a chemical reaction in which the concentrations of the reactants exhibit oscillating behavior. The Brusselator model of BZR describes the case of a single mode of oscillation to which the system returns if perturbed. The chemical reactions follow the scheme:

$$
\begin{aligned}
\mathcal{A} &\rightarrow \mathcal{X} \\
\mathcal{B} + \mathcal{X} &\rightarrow \mathcal{Y} + \mathcal{D} \\
2\mathcal{X} + \mathcal{Y} &\rightarrow 3\mathcal{X} \\
\mathcal{X} &\rightarrow \mathcal{E}
\end{aligned}
$$

where $\mathcal{A}$, $\mathcal{B}$, $\mathcal{D}$, $\mathcal{E}$, $\mathcal{X}$, and $\mathcal{Y}$ are chemical compounds. Let x and y be the concentration of compounds $\mathcal{X}$ and $\mathcal{Y}$ and A and B the concentrations of compounds $\mathcal{A}$ and $\mathcal{B}$. Assuming that the concentration A and B are held constant during the chemical reaction and that the system has only one spatial dimension one obtains the following system of differential equations

(2.7.12)
$$
\begin{aligned}
\frac{\partial x}{\partial t} &= A - (B+1)x + x^2 y + D_1 \frac{\partial^2 x}{\partial \xi^2} \\
\frac{\partial y}{\partial t} &= Bx - x^2 y + D_2 \frac{\partial^2 y}{\partial \xi^2}
\end{aligned}
$$

where D_1 and D_2 are diffusion constants and ξ is the spatial coordinate.

2.8. Bistable transmission lines [22].

One can simulate an active transition line with two stable equilibrium states in the following way. Consider a circuit which consists of a power source E_0, resistance R, capacitor C, and tunnel diode with characteristic curve $f(v)$ to be a cubic polynomial (see Figure 2). One can set E_0 and R such that the circuit acts as a bistable circuit. The equations of the circuit are given by

$$
\begin{aligned}
j &= C\frac{dv}{d\tau} + g(v), \\
g(v) &= f(v) + \frac{v - E_0}{R},
\end{aligned}
$$

where j is the current and v the potential; the function $g(v)$ is a cubic polynomial,

$$
g(v) = a(v - v_1)(v - v_2)(v - v_3),
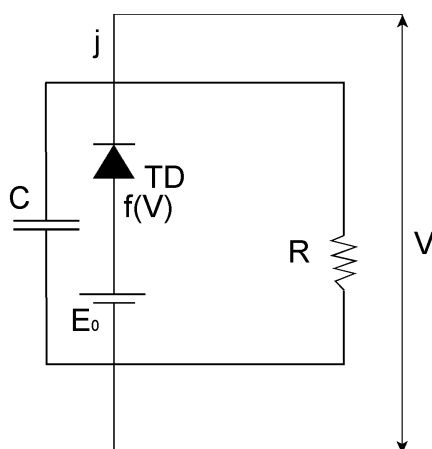$$

where $a > 0$ and $v_1 < v_2 < v_3$.
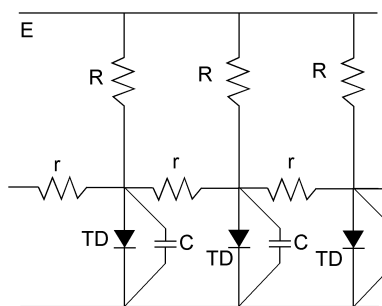
FIGURE 2. The circuit of the simple bistable line.

FIGURE 3. The distributed bistable line.

Regarding this circuit as a distributed line (see Figure 3) we obtain

$$j = \frac{1}{r}\frac{\partial^2 v}{\partial s^2},$$

where s is the distance along the line and r the interstage coupling resistance per unit length of the line. By appropriate change of variables we obtain

$$(2.8.13) \qquad \frac{\partial u}{\partial t} = -(u+1)(u-\theta)(u-1) + \kappa\frac{\partial^2 u}{\partial s^2},$$
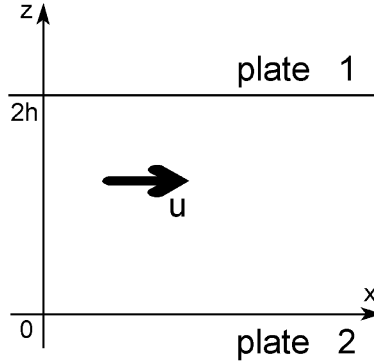
FIGURE 4. The plane Poiseuille flow.

where θ, $-1 < \theta < 1$ and κ are parameters of the circuit and u the rescaled voltage.

2.9. **Wave system in plane Poiseuille flow** [28]**.** The *Poiseuille flow* is a planar flow of an incompressible viscous fluid under pressure in a channel made up by two parallel plates with distance $2h$ between them (see Figure 4). Under the uniform pressure gradient the flow produces a velocity field which is independent of the x coordinate and has its maximum value u_0 at the center of the channel. The governing equation of the flow is

$$(2.9.14) \qquad \zeta_t + \psi_z \zeta_x - \psi_x \zeta_z = \frac{1}{R} \triangle \zeta,$$

where $R = \frac{1}{\gamma} u_0 h$ is the Reynolds number, γ the kinetic viscosity, $\psi = \psi(x, z, t, R)$ the stream function, $\zeta = -\triangle \psi$, x the direction parallel to the plates, and z the direction perpendicular to the plates. The time is measured in $\frac{h}{u_0}$ units, the length in h units, and the velocity in u_0 units. For the incompressible flow (i.e. $\nabla \vec{u} = 0$) the stream function ψ is defined by

$$\vec{u} = \nabla^\perp \psi,$$

where $\vec{u}$ is the velocity field and $\nabla^\perp := (\partial_z, -\partial_x)$.

In the case of the undisturbed laminar flow (called the *basic flow*) the motion is parallel to the plates and is given by the mean velocity with respect to x

$$\bar{u}_\ell := \frac{\partial \psi_\ell}{\partial z} = 1 - z^2,$$

where ψ_ℓ is the stream function of the undisturbed laminar flow.

Consider a small disturbance which is confined to a small neighborhood of the origin at $t = 0$. Linearization of the (2.9.14) around

the basic flow gives the following equation for the perturbed stream function ψ

$$(2.9.15) \qquad \left(\frac{\partial}{\partial t} + (1 - z^2)\frac{\partial}{\partial x} \right) \triangle \psi + 2\frac{\partial \psi}{\partial x} = \frac{1}{R}\triangle^2 \psi.$$

One can obtain a formal solution of (2.9.15) using the Fourier-Laplace transform

$$\hat{\psi}(z, \alpha, s, R) \;=\; \int_0^\infty e^{-st}dt \int_{\mathbb{R}} e^{-i\alpha x}\psi(x, z, t, R)dx,$$

$$\psi(x, z, t, R) = \psi(z) \;=\; \frac{1}{4\pi^2 i}\int_{\mathbb{R}} e^{\alpha i x}d\alpha \int_{\gamma-i\infty}^{\gamma+i\infty} e^{st}\hat{\psi}(z, \alpha, s, R)ds.$$

where the line $\mathrm{Re}(s) = \gamma$ lies to the right of all singularities of $\hat{\psi}$. Solving the above equation for ψ leads to the Orr-Sommerfeld eigenvalue problem

$$-i\alpha \left(\left(1 - z^2 - \frac{is}{\alpha} \right) \left(\frac{d\hat{\psi}^{(2)}}{dz^2} - \alpha^2\hat{\psi} \right) + 2\hat{\psi} \right)$$

$$+ \frac{1}{R}\left(\frac{d\hat{\psi}^{(4)}}{dz^4} - 2\alpha\frac{d\hat{\psi}^{(2)}}{dz^2} + \alpha^4\hat{\psi} \right) = 0.$$

Fix R and let $s(\alpha)$ be the eigenvalues of the non-trivial solution. One can show that there is a critical value R_c such that for all $R < R_c$, the real part of each eigenvalue $s(\alpha)$ is less than zero and for $R > R_c$ there are eigenvalues with positive real part. Hence, for $R > R_c$ the basic flow is unstable under the small disturbances and for $R < R_c$ it is stable.

The experiments however, show that even for $R < R_c$ the basic flow can be unstable. Thus the linear analysis is not sufficient to study stability of the basic flow and some non-linear terms should be taken into account.

For that we consider a small perturbation of the basic flow whose Reynolds number R is sufficiently close to the critical value R_c. We then expand solutions into powers of $R - R_c$ and study the leading Fourier mode of the expansion. One can show that its amplitude A satisfies the following equation

$$(2.9.16) \qquad A_t = kA|A|^2 + \varepsilon A + aA_{xx},$$

where $|\varepsilon| \ll 1$ and k, a are complex parameters; moreover, $\varepsilon > 0$ if $R > R_c$ and $\varepsilon < 0$ otherwise.
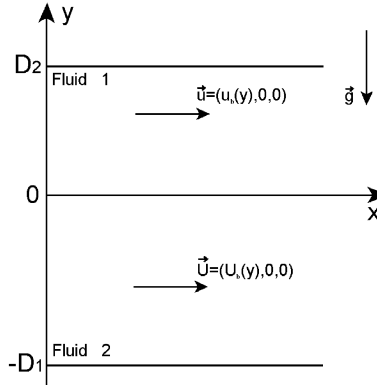
FIGURE 5. Steady state - the basic flow.

2.10. **Generating waves by wind** [4]. Consider the fully developed laminar flow of two layers of fluids (e.g. air and water) confined between two infinite parallel plates (see Figure 5; the *fully developed flow* means an entirely viscous flow with velocity independent of the horizontal position). The flow is generated by the combination of a pressure gradient and the movement of the upper plate, parallel to the pressure gradient, relative to the lower plate. Fluids are assumed to be immiscible, and in steady states the interface between two fluids is parallel to the boundary plates.

The fluids are governed by the *Naiver-Stokes equations*

(2.10.17)
$$\frac{\partial}{\partial t} + \vec{V} \cdot \nabla \vec{V} + \nu_2 \triangle \vec{V} = -\frac{2}{\rho_1} D\tilde{P} + \vec{g},$$
$$\frac{\partial}{\partial t} + \vec{v} \cdot \nabla \vec{v} + \nu_1 \triangle \vec{v} = -\frac{1}{\rho_1} D\tilde{p} + \vec{g}.$$

Here (x, y, z) is a position vector with x-axis being parallel to the plates and in the direction of the flow and y-axis perpendicular to the plates in the direction opposite to the acceleration of the gravity $\vec{g}$; $\vec{V} = (V_1, V_2, V_3)$ and $\vec{v} = (v_1, v_2, v_3)$ are velocity vectors for the upper and lower fluids; ρ_1 and ρ_2 their (constant) densities; ν_1 and ν_2 their (constant) kinematic viscosities; $\tilde{P}$ and $\tilde{p}$ the pressures applied to the lower and upper fluids.

We begin by describing the *basic flow*, that is, a steady fully developed laminar flow parallel to the plates (i.e. $\vec{V} = (V_1(y), 0, 0)$ and $\vec{v} = (v_1(y), 0, 0)$) with the boundary conditions $V_1(D_1) = V_{top}$ and $V(-D_2) = 0$ (these conditions guarantee that there is no slip on the upper and lower plates and across the interface between two fluids the velocity field is continuous). The governing equations of the basic flow

are

$$0 = \frac{G}{\rho_2} + \nu_2 \frac{d^2 V_1}{dy^2},$$

$$0 = \frac{G}{\rho_1} + \nu_1 \frac{d^2 v_1}{dy^2},$$

where

$$\frac{\partial P}{\partial x} = \frac{\partial p}{\partial x} = -G$$

is the constant pressure gradient and $p = \tilde{p} + \rho_1 gy$ and $P = \tilde{P} + \rho_2 gy$ are modified pressures. Let $\tilde{V}_b(y)$, $\tilde{v}_b(y)$, P_b, p_b be the solution of this system (with boundary conditions discussed above). These solutions depend linearly on G and V_{top}. We introduce the dimensionless velocities

$$V_b = \frac{\tilde{V}_b}{V_{mean}}, \quad v_b = \frac{\tilde{v}_b}{V_{mean}},$$

where V_{mean} is the mean velocity

$$V_{mean} = \frac{1}{D_1 + D_2} \left(\int_{-D_1}^{0} \tilde{v}_b dy + \int_{0}^{D_2} \tilde{V}_b dy \right).$$

We also introduce the *Reynolds number* $R = \frac{V_{mean} D_2}{\nu_2}$.

The "wind" can be viewed as a perturbation of the basic flow for which the velocity field can be represented in the form

$$\vec{v} = (v_b, 0, 0) + \delta \cos(kx + lz - kct) (v_1(y), v_2(y), v_3(y)),$$

$$\vec{V} = (V_b, 0, 0) + \delta \cos(kx + lz - kct) (V_1(y), V_2(y), V_3(y)),$$

and the pressures

$$p = p_b + \delta p(y) \cos(kx + lz - kct),$$

$$P = P_b + \delta p(y) \cos(kx + lz - kct).$$

Here $\delta \ll 1$, $k, l \in \mathbb{C}$ are *disturbance wave numbers* in x- and z-directions respectively, and $c \in \mathbb{C}$ the phase speed. This kind of perturbation is considered frequently in the systems with translational invariance. It corresponds to the study of the stability of the Fourier modes (which represents delocalized disturbances) ([7]).

The perturbed system is governed by the Navier-Stokes equation (2.10.17) with boundary conditions as above and the velocity field being continuous across the interface $y = \eta(x, z, t)$ where

$$\eta(x, z, t) = \delta \cos(kx + lz - kct).$$

To study stability of the basic flow we substitute the values of pressures and velocities into (2.10.17) and linearize this system along the

basic flow. One can show that in the (R, k)-plane there exists the *stability curve*, i.e., a curve that divides the (R, k)-plane into two regions in which the basic flow is stable and unstable respectively. This curve has a critical point (R_c, k_c) for which $k_c \neq 0$.

Now, consider a small perturbation of the basic flow whose Reynolds number R is sufficiently close to the critical value R_c. By expanding solutions of (2.10.17) into powers of $R - R_c$ one can show that

$$(2.10.18) \qquad A_t = bA + kA\,|A|^2 + aA_{xx},$$

where A is the leading Fourier mode of the expansion (i.e. amplitude of the surface wave is proportional to A), a a complex parameter with positive real part, b a complex parameter which is related to the exponential growth of the wave for $R > R_c$, and k is a complex parameter which is related to the motion in the bulk of the fluid and nonlinear effects at the interface.

3. A CLASSIFICATION OF MODELS.

A non-linear reaction-diffusion equation is a PDE of the form:

$$(3.0.19) \qquad u_t(x, t) = h(u) + \mathcal{A}\kappa\Delta_x u(x, t),$$

where $u(x, t)$ is a function of space coordinate $x \in \mathbb{R}^n$ and time $t \geq 0$ with values in $\mathbb{R}^d$; $\mathcal{A}$ is the coupling matrix, and κ a diffusion coefficient. One can obtain a number of well-known equations by the appropriate choice of the nonlinear term h.

3.1. **The Kolmogorov-Petrovsky-Piskunov (KPP) Equation.** The Fisher linear model and the KPP planar model of advance of advantageous genes (Equations (2.3.4) and (2.2.3)) are examples of the generalized KPP equation introduced in [16]. This is a one-dimensional reaction-diffusion equation

$$(3.1.20) \qquad u_t(x, t) = h(u) + \kappa\triangle u(x, t), \quad 0 \leq u \leq 1,$$

where the nonlinear term $h(u) \in C^1([0, 1])$ satisfies the following conditions:

$$(3.1.21) \quad h(0) = h(1) = 0, \quad h'(0) = \alpha > 0, \quad h'(u) < \alpha, \quad u \in (0, 1],$$

For the Fisher model we have $h(u) = \alpha u(1 - u)$ and for the KPP model $h(u) = \alpha u(1 - u)^2$.

3.2. **The FitzHugh-Nagumo Equation.**   The FitzHugh model of propagation of voltage impulse through a nerve axon (Equation (2.6.10)) and Maginu model of morphogenesis (Equation (2.5.6)) are described by the FitzHugh-Nagumo generalized equation. It is a two dimensional reaction-diffusion equation with $u(x,t) = (u_1(x,t), u_2(x,t))$, $x \in \mathbb{R}$ and

$$h(u_1, u_2) = (n(u_1) - bu_2, cu_1 - du_2),$$

$$\mathcal{A} = \begin{pmatrix} \sigma_1 & 0 \\ 0 & \sigma_2 \end{pmatrix},$$

where a, b, c, d, and σ_i are positive parameters, $\sigma_i \in \{0, 1\}$, $i = 0, 1$, and

$$n(u_1) = -au_1(u_1 - \theta)(u_1 - 1)$$

with $\theta \in (0, 1)$. The equations become

(3.2.22)
$$\frac{\partial u_1}{\partial t} = -au_1(u_1 - \theta)(u_1 - 1) - bu_2 + \kappa_1 \frac{\partial^2 u_1}{\partial x^2}$$
$$\frac{\partial u_2}{\partial t} = cu_1 - du_2 + \kappa_2 \frac{\partial^2 u_2}{\partial x^2}.$$

where $\kappa_i \geq 0$ and at least one of them is nonzero.

3.3. **Nagumo Equation.** The one-dimensional FitzHugh model of propagation of voltage impulse through a nerve axon (Equation (2.6.11)), the Fisher model in population genetics (Equation (2.1.1)), and bistable transition lines (Equation (2.8.13)) are described by the Nagumo equation. The latter is a special case of the more general semi-linear bistable reaction-diffusion equation

(3.3.23)
$$u_t(x, t) = h(u) + \kappa u_{xx}(x, t),$$

where the nonlinear term is given by

$$h(u) = -au(u - \theta)(u - 1),$$

with $a > 0$ and $\theta \in (0, 0.5]$. Note that the case $\theta \in (0.5, 1)$ can be reduced to the previous one by replacing u with $-u + 1$. Also note that Equation (3.3.23) is the first equation in the system (3.2.22) for $b = 0$.

3.4. **The Real Ginzburg-Landau (Amplitude) Equation.** The amplitude of the disturbance in the Poiseuille flow (Equation 2.9.16) and amplitude of the waves generated by wind (Equation 2.10.18) are all described by the amplitude equation. A general complex Ginzburg-Landau equation is given by

$$u_t(x, t) = \beta u |u|^2 - \gamma u + \alpha \Delta_x u(x, t),$$

where $\alpha, \beta \in \mathbb{C}$, and $\gamma \in \mathbb{R}$ are parameters, $u \in \mathbb{C}$. Here we only consider a one dimensional real version of this equation given by

$$(3.4.24) \qquad u_t(x,t) = u(\gamma - \delta u^2) + \kappa u_{xx}(x,t),$$

where $\gamma, \delta, \kappa \in \mathbb{R}$. Note that if $\gamma, \delta, \kappa > 0$ Equation (3.4.24) becomes (after rescaling) the Nagumo equation (3.3.23).

3.5. **Some Other Non-linear Reaction-Diffusion Equations.** The Brusselator model for the Belousov-Zhabotinsky reaction (Equation 2.7.12) gives us another two dimensional reaction-diffusion equation

$$(3.5.25) \qquad \begin{aligned} \frac{\partial u_1}{\partial t} &= A - (B+1)u_1 + u_1^2 u_2 + \kappa_1 \frac{\partial^2 u_1}{\partial x^2}, \\ \frac{\partial u_2}{\partial t} &= B u_1 - u_1^2 u_2 + \kappa_2 \frac{\partial^2 u_2}{\partial x^2}. \end{aligned}$$

where A, B, κ_i, $i = 0, 1$ are positive parameters.

Finally, from the Turing model of morphogenesis (Equation 2.4.5) we obtain yet another two dimensional system

$$(3.5.26) \qquad \begin{aligned} \frac{\partial u_1}{\partial t} &= -(a u_1^2 + b u_1 u_2) + c + \kappa_1 \frac{\partial^2 u_1}{\partial x^2}, \\ \frac{\partial u_2}{\partial t} &= (a u_1^2 + b u_1 u_2) - d u_2 + e + \kappa_2 \frac{\partial^2 u_2}{\partial x^2}. \end{aligned}$$

where a, b, c, d, e, and κ_i, $i = 0, 1$ are positive parameters.

4. Coupled Map Lattices (CML).

To construct CMLs which correspond to the PDEs described above we use the following discretization. For the derivative in time

$$\frac{\partial u(x,t)}{\partial t} \to \frac{u(x, t + \Delta t) - u(x,t)}{\Delta t}.$$

For the space derivative one can choose any discretization method involving an arbitrary number of points. For example,

$$\begin{aligned} \frac{\partial u(x,t)}{\partial x} &\to \frac{u(x + \Delta x, t) - u(x,t)}{\Delta x} \\ \frac{\partial u^2(x,t)}{\partial x^2} &\to \frac{u(x + \Delta x, t) - 2u(x,t) + u(x - \Delta x, t)}{(\Delta x)^2}, \end{aligned}$$

where Δt and Δx are the discretization steps.

Using the above discretization we obtain the CMLs corresponding to the above mentioned PDEs. We describe below the local maps for these CMLs and indicate leading parameters, i.e., the parameters that we will vary to obtain different types of dynamics.

- The KPP equation:

$$f(u) = u + \gamma h(u),$$

where $h(u)$ satisfies (3.1.21), $h'(0) = \alpha$ is a leading parameter and $\gamma = \Delta t > 0$ is a parameter.

- The Nagumo equation:

$$f(u) = u - Au(u - \theta)(u - 1),$$

where $A = \alpha \Delta t > 0$ is a leading parameter and $\theta \in (0, 0.5)$ is a parameter.

- The real amplitude equation:

$$f(u) = Au - bu^3,$$

where $A = (1 + \gamma \Delta t) > 0$ is a leading parameter and $b = \delta \Delta t \in \mathbb{R}$ is a parameter.

- The FitzHugh-Nagumo equation:

$$f(u_1, u_2) = (u_1 - Au_1(u_1 - \theta)(u_1 - 1) - \alpha u_2, \beta u_1 + \gamma u_2),$$

where $A = a \triangle t > 0$ is a leading parameter, $\alpha = b \triangle t > 0$, $\beta = c \triangle t > 0$, $\gamma = (1 - d \triangle t) > 0$, $\theta \in (0, 1)$ are parameters.

- The Brusselator model:

$$f(u_1, u_2) = (a + (1 - \gamma - b)u_1 + \gamma u_1^2 u_2, u_2 + bu_1 - \gamma u_1^2 u_2),$$

where $a = A \triangle t > 0$, $b = B \triangle t > 0$ are two leading parameters, and $\gamma = \triangle t > 0$ is a parameter.

- The Turing model:

$$f(u_1, u_2) = (u_1 - Au_1^2 - Bu_1 u_2 + C,$$
$$Au_1^2 + Bu_1 u_2 + (1 - D)u_2 + E),$$

where $A = a \triangle t > 0$, $B = b \triangle t > 0$, $C = c \triangle t > 0$, $D = d \triangle t > 0$, and $E = e \triangle t > 0$ are parameters.

The interaction g is a function of $2s + 1$ variables, where in our case $s = 1$.

5. Dynamics of Local Map: One Dimensional Maps.

We consider the case of one-dimensional local maps. We show that in some range of parameters they exhibit Morse-Smale type behavior.

5.1. **KPP Equation.** We begin with the KPP equation and consider local maps of two types: (1) $f(u) = u + \gamma u(1 - u)$ and (2) $f(u) = u + \gamma u(1 - u)^2$.
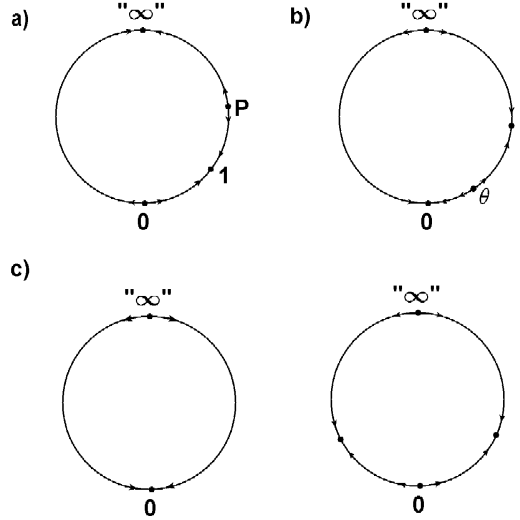
FIGURE 6. Phase Portraits of 1-dimensional maps: a) KPP equation, $f(u) = u + \gamma u(1 - u), 0 < \gamma < 1$; b) Nagumo equation, $f(u) = u - Au(u - \theta)(u - 1), A < 1$; c) real amplitude equation, $f(u) = Au - bu^3$.
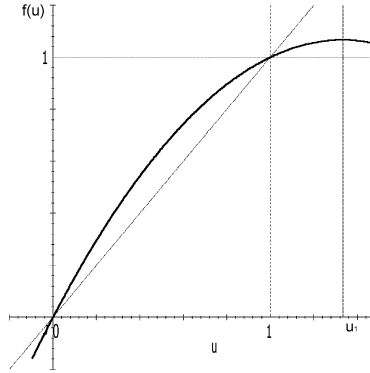

FIGURE 7. The local map of the KPP equation, $f(u) = u + \gamma u(1 - u)$, $\gamma < 1$.

5.1.1. *The local map $f(u) = u + \gamma u(1 - u)$.* Assume that $0 < \gamma < 1$ and let $u_1 = \frac{1}{2} + \frac{1}{2\gamma} > 1$. The derivative $f'(u) = 1 + \gamma(1 - 2u) > 0$ for $u < u_1$ while $f'(u_1) = 0$ (see Figure 7). The local map has two fixed points: $u = 0$ is repelling $(f'(0) = 1 + \gamma > 1)$ and $u = 1$ is attracting $(f'(1) = 1 - \gamma < 1)$. We change f outside of $[0, u_1]$ such that the new map (still called f) has a repelling fixed point $u = P$ and $f'(u) > 0$
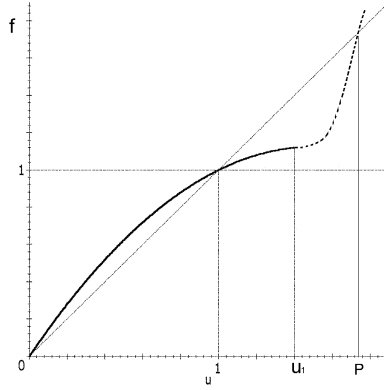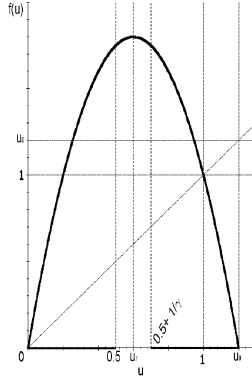
FIGURE 8. The modified local map of the KPP equation.

FIGURE 9. The local map of the KPP equation, $f(u) = u + \gamma u(1 - u)$, $\gamma > 1 + \sqrt{5}$.

for all $u \in \mathbb{R}$ and $f'(u) > 1$ for $u > P$ (see Figure 8). The new map is a diffeomorphism of $\mathbb{R}$ with three fixed points and no other periodic points. Let $\tilde{f}$ be the compactification map of f (see Appendix).

Theorem 5.1.1. *For all $\gamma \in (0, 1)$ the compactification map $\tilde{f}$ is a Morse-Smale diffeomorphism of S^1 with four fixed points corresponding to $\{0, 1, p, \infty\}$ (see Figure 6(a)).*

We now consider the KPP equation for the sufficiently large γ (see Figure 9). Set $u_0 = 2u_1 = 1 + \frac{1}{\gamma}$. It is clear that $f(0) = f(u_0) = 0$, $f(u_1) > u_0$ if $\gamma > 3$. Since $f'(u) = 1 + \gamma - 2\gamma u$ we obtain $f'(\frac{1}{2}) = 1$ and $f'(\frac{1}{2} + \frac{1}{\gamma}) = -1$. One also has $f(\frac{1}{2}) = f(\frac{1}{2} + \frac{1}{\gamma}) > u_0$ if $\gamma > 1 + \sqrt{5}$. It follows that for any small $\varepsilon > 0$ there exists $\lambda = \lambda(\varepsilon) > 1$ such that $|f'(u)| \geq \lambda$ for any $u \in [0, \frac{1}{2} - \varepsilon] \cup [\frac{1}{2} + \varepsilon + \frac{1}{\gamma}, u_0]$, i.e., the map f is expanding.
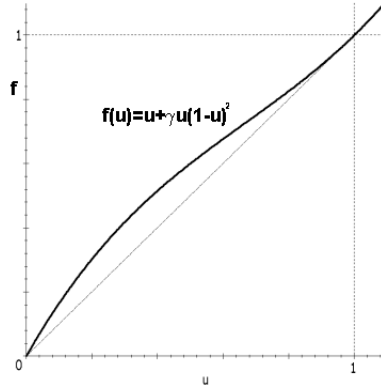
FIGURE 10. The local map of the KPP equation, $f(u) = u + \gamma u(1-u)^2$.

Theorem 5.1.2. *Assume that $\gamma > 1 + \sqrt{5}$ and let*

$$U = [0, \frac{1}{2}] \cup [\frac{1}{2} + \frac{1}{\gamma}, 1 + \frac{1}{\gamma}].$$

Then the set

$$\Lambda = \bigcap_{n \geq 0} f^{-n}(U)$$

is a Cantor-like subset of U on which f is conjugate to the full shift on the space Σ_2^+ of one-sided infinite binary sequences.

5.1.2. *The local map $f(u) = u + \gamma u(1-u)^2$.* Assume that $\gamma > 0$. The local map $f(u) = u + \gamma u(1-u)^2$ has two fixed points on $[0,1]$ (see Figure 10): $u = 0$ is repelling ($f'(0) = 1 + \gamma > 1$) and $u = 1$ is neutral ($f'(1) = 1$). It is easy to check that if $\gamma > 0$ and $u \in (-\infty, \frac{1}{3}) \cup (1, +\infty)$ we have $f'(u) > 1$ and hence $f(u)$ is expanding on $(-\infty, 0) \cup (1, +\infty)$ so there are only two fixed points for all $u \in \mathbb{R}$. Hence, for $0 < \gamma < 1$ map $f(u)$ is a homeomorphism of $\mathbb{R}$ with two fixed points and it is easy to see that there are no other periodic points. The compactification map $\tilde{f}$ has three fixed points: points corresponding to 0 and ∞ are hyperbolic and point corresponding to $u = 1$ is neutral. The phase portrait of $\tilde{f}$ resembles the phase portrait of a Morse-Smale map (see Figure 6).

5.2. **Nagumo Equation.** The local map is a cubic polynomial, $f(u) = u - Au(u - \theta)(u - 1)$ (see Figure 11). It has three fixed points $\{0, \theta, 1\}$
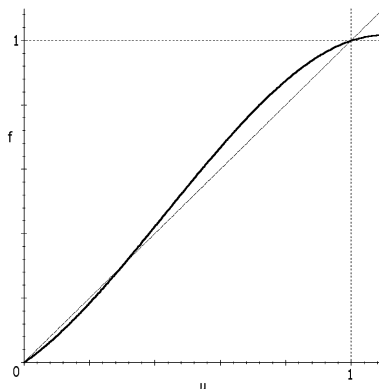
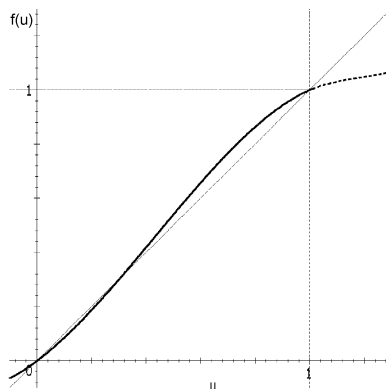FIGURE 11. The local map of the Nagumo equation, $f(u) = u - Au(u - \theta)(u - 1)$.

FIGURE 12. The modified local map of the Nagumo equation.

which are hyperbolic for sufficiently small A:

$$\begin{aligned} |f'(0)| &= |1 - A\theta| < 1, \\ |f'(\theta)| &= |1 + A\theta(1 - \theta)| > 1, \\ |f'(1)| &= |1 - A(1 - \theta)| < 1. \end{aligned}$$

The derivative $f'(u) = 1 + Ah(u)$, where $h(u) = -3u^2 + 2(\theta + 1)u - \theta$.

We modify the map f outside some large interval $[-R, R]$, $R \gg 1$, such that the new map $\hat{f}$ satisfies the following conditions:

(1) $\hat{f}(x) = f(x)$ for $x \in [-R, R]$;
(2) for $x \in \mathbb{R}\backslash[-R, R]$ map $\hat{f}(x)$ is as on Figure 12;
(3) $\hat{f} \in C^2(\mathbb{R})$, moreover $\hat{f}'$ and $\hat{f}''$ are bounded on $\mathbb{R}$;
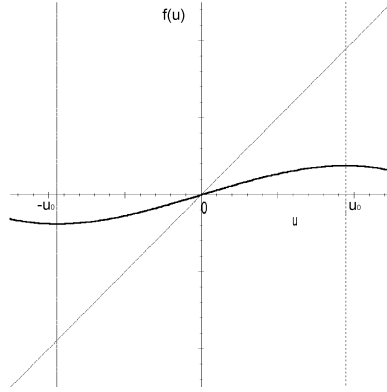(4) $\lim_{x \to -\infty} \hat{f} = -\infty$ and $\lim_{x \to +\infty} \hat{f} = +\infty$.

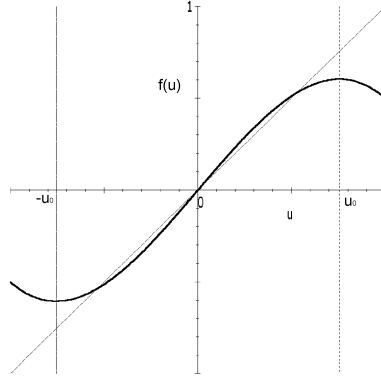FIGURE 13. The local map of the Real Amplitude Equation, $f(u) = Au - bu^3$, $A \in (0, 1)$.

FIGURE 14. The local map of the Real Amplitude Equation, $f(u) = Au - bu^3$, $A \in (1, \frac{3}{2})$.

Theorem 5.2.1. *For all sufficiently small A the compactification map $\tilde{f}$ is a Morse-Smale diffeomorphism of S^1 with four fixed points corresponding to $\{0, \theta, 1, \infty\}$ (see Figure 6(b)).*

5.3. **Real Amplitude Equation.** The local map is a cubic polynomial, $f(u) = Au - bu^3$. Let $A \in (0, 1) \cup (1, \frac{3}{2})$ and $b > 0$. The map f is an endomorphism with one fixed point 0 if $A < 1$ (see Figure 13) and three fixed points $\{0, \pm\sqrt{\frac{A-1}{b}}\}$ if $A \in (1, \frac{3}{2})$ (see Figure 14). All fixed points are hyperbolic.

Set $u_0 = \sqrt{\frac{A}{3b}}$, then $f'(u_0) = 0$. Let $R = u_0 - \epsilon$ for sufficiently small ϵ. We can change f outside of $[-R, R]$ in such a way that the new map f has $f'(u) > 0$ for $u \in \mathbb{R}$ (here we need $A < \frac{3}{2}$) and $f'(u) < 1$ for $u \in \mathbb{R}\backslash[-R, R]$. The new map is a diffeomorphism of $\mathbb{R}$ with four
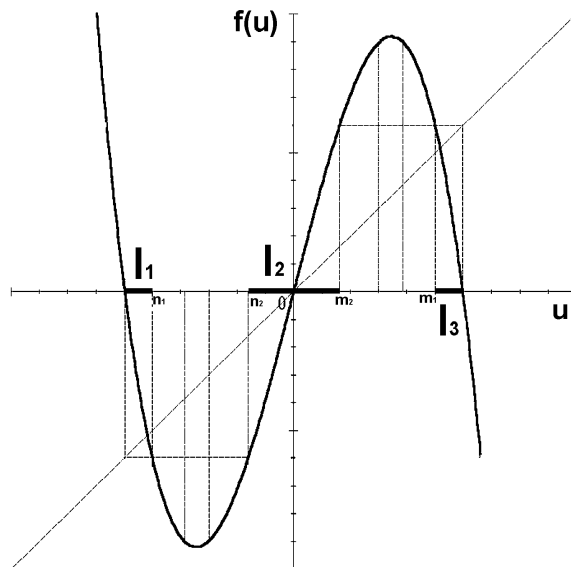
FIGURE 15. The local map of the Real Amplitude Equation, $f(u) = Au - bu^3$, $A > 3$.

hyperbolic fixed points (one of them being ∞) if $A \in (1, \frac{3}{2})$ and two hyperbolic fixed points if $A \in (0, 1)$. The map has no other periodic points.

Theorem 5.3.1. *For $b > 0$ and $A \in (0, 1) \cup (1, \frac{3}{2})$ the compactification map $\tilde{f}$ is a Morse-Smale diffeomorphism of S^1 with four fixed points if $A \in (1, \frac{3}{2})$ and two fixed points if $A \in (0, 1)$ (see Figure 6(c)).*

We now consider the real amplitude equation for large values of A. For $A > \frac{3\sqrt{3}}{2}$ the local maximum and minimum exceed, in absolute value, $\sqrt{\frac{A}{b}}$, where $f(\sqrt{\frac{A}{b}}) = f(-\sqrt{\frac{A}{b}}) = 0$ (see Figure 15). Let $m_1 > m_2 > 0$ be two positive solutions of the equation

$$f(x) = \sqrt{\frac{A}{b}}$$

and $n_1 < n_2 < 0$ two negative solutions of the equation

$$f(x) = -\sqrt{\frac{A}{b}}.$$

Set $I_1 = [-\sqrt{\frac{A}{b}}, n_2]$, $I_2 = [n_2, m_2]$, and $I_3 = [m_1, \sqrt{\frac{A}{b}}]$. One has

$$|f'(\sqrt{\frac{A-1}{3b}})| = |f'(-\sqrt{\frac{A-1}{3b}})| =$$
$$|f'(\sqrt{\frac{A+1}{3b}})| = |f'(-\sqrt{\frac{A+1}{3b}})| = 1,$$

and for $A > 3$ a straightforward computation shows that $m_2 < \sqrt{\frac{A-1}{3b}}$. Hence, the following is true

(1) $|f'(x)| > 1$ for $x \in I_i$, $i = 1, 2, 3$;
(2) $f^{-1}\left([-\sqrt{\frac{A}{b}}, \sqrt{\frac{A}{b}}]\right) = I_1 \cup I_2 \cup I_3$.

Let

$$\Lambda = \bigcap_{i \geq 0} f^{-i}\left([-\sqrt{\frac{A}{b}}, \sqrt{\frac{A}{b}}]\right).$$

The following is the well known fact for the cubic non-linearity:

Theorem 5.3.2. *If $A > 3$ then $f|_\Lambda$ is conjugated to the Markov chain $\Omega|_\mathcal{B}$, where*

$$\mathcal{B} = \begin{pmatrix} 1 & 1 & 0 \\ 1 & 1 & 0 \\ 0 & 1 & 1 \end{pmatrix}.$$

6. Dynamics of the Local Map for the FitzHugh-Nagumo Equation.

In this section we present rigorous and numerical results for the local map for the FitzHugh-Nagumo equation (which is a two-dimensional equation).

6.1. **Rigorous Results.** The local map is given by

$$f(u_1, u_2) = (u_1 - Au_1(u_1 - \theta)(u_1 - 1) - \alpha u_2, \beta u_1 + \gamma u_2),$$

where $A, \alpha, \beta > 0$, $\gamma \in (0, 1)$, and $\theta \in (0, 1)$ are parameters. We modify the cubic nonlinear term in u_1-coordinate outside some large interval $[-R, R]$ as in Section 5.2 (and we still call this map f). We also consider the compactification map $\tilde{f}$ on S^2.

We will show that: 1) for all sufficiently large values of A the map f posses a Smale horseshoe, 2) for all sufficiently small values of A the compactification map $\tilde{f}$ is of Morse-Smale type, and 3) for intermediate values of A the map f a trapping region and a "strange" attractor. We believe that for some values this attractor is Hénon-like.
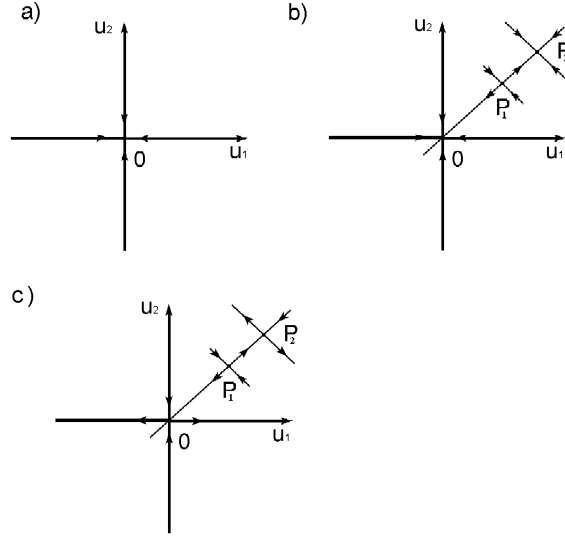
FIGURE 16. The local map for the FitzHugh-Nagumo equation with: a) one attracting fixed point; b) two attracting fixed points and one saddle; c) three saddles.

It is easy to check that the map f has one fixed point, $O = (0,0)$, if

$$(6.1.27) \qquad A < \frac{4\alpha\beta}{(1-\gamma)(1-\theta)^2}$$

and three fixed points, $O = (0,0)$ and $P_i = (x_i, y_i)$, $i = 1, 2$, where

$$(6.1.28) \quad x_i = \frac{1}{2}\left(\theta + 1 \mp \sqrt{(\theta-1)^2 - \frac{4\alpha\beta}{A(1-\gamma)}}\right), \quad y_i = \frac{\beta}{1-\gamma}x_i,$$

if

$$(6.1.29) \qquad A > \frac{4\alpha\beta}{(1-\gamma)(1-\theta)^2}.$$

Theorem 6.1.1. *There exist positive α_0, β_0, and A_0 such that if*

$$0 < A < A_0, \quad 0 < \alpha < \alpha_0, \quad 0 < \beta < \beta_0, \quad 0 < \theta < 1, \quad 0 < \gamma < 1,$$

and

$$A \neq \frac{4\alpha\beta}{(1-\gamma)(1-\theta)^2},$$

the compactification map $\tilde{f}$ is a Morse-Smale diffeomorphism of the sphere S^2. Moreover,

(1) *if (6.1.27) holds then the map $\tilde{f}$ has two fixed points corresponding to 0 (attracting) and ∞ (repelling) (see Figure 16(a));*
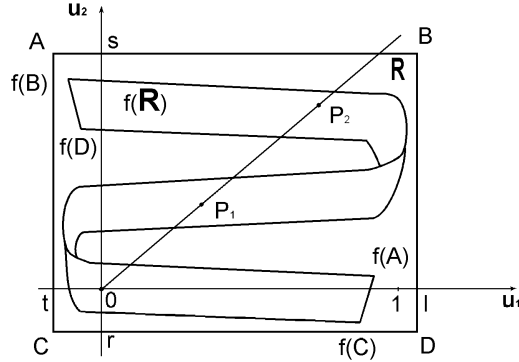
FIGURE 17. The attractor for the FitzHugh-Nagumo map: the first image of the rectangle $\mathbf{R}$.

(2) *if (6.1.29) holds then the map $\tilde{f}$ has four fixed points corresponding to $0 = (0,0)$ (attracting), ∞ (repelling), $P_1 = (x_1, y_1)$ (saddle), and $P_2 = (x_2, y_2)$ (attracting) (see Figure 16(b)).*

Proof. We write the map f in the form

$$f(u_1, u_2) = f_0(u_1, u_2) + f_1(u_1, u_2),$$

where $f_1(u_1, u_2) = (-\alpha u_2, \beta u_1)$, $f_0(u_1, u_2) = (u_1 - Au_1(u_1 - 1)(u_1 - \theta), \gamma u_2)$ on $[-R, R]$, and $f_0(u_1, u_2)$ is modified as above for $x \in \mathbb{R} \backslash [-R, R]$. Let $\tilde{f}_0$ be the compactification of the map f_0. We have that $\tilde{f} = \widetilde{f_0 + f_1}$ is a small pertrubation of $\tilde{f}_0$ for sufficiently small α and β. It follows from Sec. 5.2 that for $\gamma \in (0, 1)$ and all sufficiently small A, the map $\tilde{f}_0$ is a Morse-Smale diffeomorphism of S^2. The theorem follows from the structural stability of Morse-Smale systems (i.e., a small perturbation of a Morse-Smale diffeomorphism is again a Morse-Smale diffeomorphism; see [25]). $\qquad \square$

Theorem 6.1.2. *There exist a rectangle $\mathbf{R} = [t, \ell] \times [r, s] \subset \mathbb{R}^2$ (for some $\ell > 1 > 0 > t$ and $s > 0 > r$) and numbers*

$$\alpha_0 > 0, \ 0 < A_2 < A_3, \ 0 < \theta_1 < \frac{1}{2} < \theta_2 < 1$$

such that if

$$0 < \gamma < 1, \ 0 < \alpha < \alpha_0, \ 0 < \beta, \ \theta_1 < \theta < \theta_2, \ A_2 < A < A_3,$$

then

(1) *condition (6.1.29) holds, the three fixed points, $O = (0,0)$ and $P_i = (x_i, y_i)$, $i = 1, 2$, are saddles, and they lie inside* **R** *(see Figure 16(b,c));*

(2) $\overline{f(\mathbf{R})} \subset \mathbf{R}$, *i.e.* **R** *is a trapping region (see Figure 17).*

It follows immediately that the map f has an attractor

$$\Lambda = \bigcap_{n \geq 0} f^n(\mathbf{R}).$$

The structure of this attractor will be discussed in the next section.

Proof. Let $\mathbf{R} = [t, \ell] \times [r, s] \subset \mathbb{R}^2$, $\ell > 1 > 0 > t$, $s > 0 > r$, be a rectangle.

We require that the image of the point $\mathbf{B} = (\ell, s)$ lie below the line $u_2 = s$ and the image of the point $\mathbf{C} = (t, r)$ above the line $u_2 = r$, i.e.,

$$\beta \ell + \gamma s < s, \quad \beta t + \gamma r > r.$$

Hence,

(6.1.30) $$s > \frac{\beta \ell}{1 - \gamma}, \quad r < \frac{\beta t}{1 - \gamma}.$$

In what follows we choose $|\ell| < 2$ and $|t| < 1$. Therefore, (6.1.30) can be assured by any choice of $\beta > 0$ and $0 < \gamma < 1$.

The images of the horizontal edges of the rectangle **R** are

$$f(\mathbf{AB}) = (k(u_1) - \alpha s, \beta u_1 + \gamma s),$$

$$f(\mathbf{CD}) = (k(u_1) - \alpha r, \beta u_1 + \gamma r),$$

for $u_1 \in [t, \ell]$, where $k(u_1) = u_1 - A u_1 (u_1 - \theta)(u_1 - 1)$. We require that the images of **AB** and **CD** lie in **R** , i.e., for $u_1 \in (t, \ell)$, one must have

(6.1.31) $$t < k(u_1) - \alpha s < k(u_1) - \alpha r < \ell.$$

We want to show that one can choose ℓ and t, such that (6.1.31) hold for an appropriate choice of parameters A, θ, and α.

We first consider the case when $\alpha = 0$ and $\theta = \frac{1}{2}$. It is easy to check that for all $A > 4$ all three fixed points are hyperbolic. To guarantee (6.1.31) it is sufficient to choose ℓ and t such that

(6.1.32) $$k(c_2) < \ell, \quad k(c_1) > t,$$

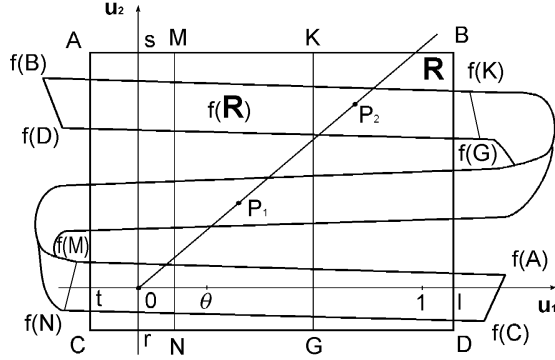(6.1.33) $$k(t) < \ell, \quad k(\ell) > t,$$

FIGURE 18. The Smale horseshoe for the FitzHugh-
Nagumo map.

where c_1 is the local minimum and c_2 is the local maximum of $k(u_1)$.
(6.1.33) can be assured by choosing A such that

$$A < \hat{A}(t,\ell) = \min\left\{\frac{\ell - t}{-t\,(t-1)\left(t - \frac{1}{2}\right)},\ \frac{\ell - t}{\ell\,(\ell - 1)\left(\ell - \frac{1}{2}\right)}\right\}.$$

Note that $\hat{A}(-0.044, 1.045) > 4$. Therefore there are t_0 and ℓ_0 such
that $\hat{A}(t,\ell) > 4$ for all $t_0 < t < -0.044$ and $1.045 < \ell < \ell_0$. On the
other hand for $A = 4$ one has

$$k(c_2) < 1.045, \quad k(c_1) > -0.044.$$

Hence, by continuity, there is $4 < \tilde{A}_3 < B$ such that inequality (6.1.32)
holds for all $4 < A < \tilde{A}_3$.

Notice that maps

$$(\alpha, \theta) \mapsto f(u_1, u_2), \quad (\alpha, \theta) \mapsto D_{(u_1, u_2)}f$$

are continuous. Therefore, there is a neighborhood of $\theta = \frac{1}{2}$, (θ_1, θ_2),
$0 < \theta_1 < \frac{1}{2} < \theta_2 < 1$, and a neighborhood of $\alpha = 0$, $(0, \alpha_0)$, $\alpha_0 > 0$,
such that there exist ℓ, t, and $A_2 < A_3$ such that estimate (6.1.31) still
holds. It follows that $\overline{f(\mathbf{R})} \subset \mathbf{R}$. $\square$

Theorem 6.1.3. *There exists a rectangle* $\mathbf{R} = [t, \ell] \times [r, s] \subset \mathbb{R}^2$ *(for
some* $\ell > 1 > 0 > t$ *and* $s > 0 > r$*) and a number* $A_4 > 0$ *such that for*

all $A > A_4$ one can find $\alpha_0 > 0$, and $\beta_0 > 0$ for which if

$$0 < \gamma < 1, \ 0 < \theta < 1, \ 0 < \alpha < \alpha_0, \ 0 < \beta < \beta_0$$

then

(1) *condition (6.1.29) holds, the three fixed points, $O = (0,0)$ and $P_i = (x_i, y_i)$, $i = 1, 2$ are saddles, and they lie inside $\mathbf{R}$ (see Figure 18);*

(2) *the set*

$$\Lambda = \bigcap_{n=-\infty}^{\infty} f^n(\mathbf{R})$$

is a locally maximal hyperbolic set for f.

Note that set Λ is a Smale horseshoe.

Proof. For for some $s > 0 > r$ and $\ell > 1 > 0 > t$ set $\mathbf{R} = [t, \ell] \times [r, s] \subset \mathbb{R}^2$. We shall show that the following statements hold:

(1) $f(\mathbf{R}) \cap \mathbf{R}$ has three disjoint connected "horizontal" components (see Figure 18);

(2) $f^{-1}(\mathbf{R}) \cap \mathbf{R}$ has three disjoint connected "vertical" components;

(3) Λ is hyperbolic;

(4) $O, P_1, P_2 \in \mathbf{R}$.

We need the following simple lemma.

Lemma 6.1.4. *Let $n(x) = -x(x-1)(x-\theta)$, $h(x) = n'(x) = -3x^2 + 2(\theta+1)x - \theta$, and $\tilde{x}_1, \tilde{x}_2$ be the roots of $h(x)$. Then*

$$0 < \tilde{x}_1 < \theta < \tilde{x}_2 < 1, \quad n(\tilde{x}_1) < 0, \quad n(\tilde{x}_2) > 0,$$

$n(x) > 0$ *for* $x \in (-\infty, 0) \cup (\theta, 1)$ *and* $n(x) < 0$ *for* $x \in (0, \theta) \cup (1, +\infty)$.

To prove Statement 1 we consider the images of the following line segments (see Figure 18):

$$AC = \{(t, u_2) | \quad u_2 \in [r, s]\},$$

$$MN = \{(k, u_2) | \quad u_2 \in [r, s]\}, 0 < k < \theta,$$

$$KG = \{(\frac{\theta+1}{2}, u_2) | \quad u_2 \in [r, s]\}, \quad BD = \{(\ell, u_2) | \quad u_2 \in [r, s]\}.$$

We have

$$f(AC) = (t - At(t-1)(t-\theta) - \alpha u_2, \beta t + \gamma u_2),$$

$$f(MN) = (k - Ak(k-1)(k-\theta) - \alpha u_2, \beta k + \gamma u_2),$$

$$f(KG) = (\frac{\theta+1}{2} + A\frac{(\theta+1)(\theta-1)^2}{8} - \alpha u_2, \ \beta\frac{\theta+1}{2} + \gamma u_2),$$

$$f(BD) = (\ell - A\ell(\ell-1)(\ell-\theta) - \alpha u_2, \beta\ell + \gamma u_2),$$

where $u_2 \in [r, s]$.

For all suficiently large values of A the line segments $f(BD)$ and $f(MN)$ lie to the left of the line $u_1 = t$ and the line segments $f(AC)$ and $f(KG)$ lie to the right of the line $u_1 = \ell$. The latter implies that

$$(6.1.34) \qquad \theta + A \frac{(\theta + 1)(\theta - 1)^2}{4} > \ell + 2\alpha s.$$

We also require that the images of four corner points A, B, C, and D lie between lines $u_2 = r$ and $u_2 = s$, i.e.,

$$(6.1.35) \qquad r < \frac{\beta t}{1 - \gamma}, \quad s > \frac{\beta \ell}{1 - \gamma}.$$

Next we want the images of the points where the map f is not locally one-to-one to lie outside of $\mathbf{R}$. We have that

$$Df_{(u_1, u_2)} = \begin{pmatrix} 1 + Ah(u_1) & -\alpha \\ \beta & \gamma \end{pmatrix},$$

where $h(u_1) = -3u_1^2 + 2(1 + \theta)u_1 - \theta$. There are two values of u_1, $u_1 = e_{1,2}$, such that $Df_{(u_1, u_2)}$ is not invertible:

$$e_{1,2} = \frac{1}{3}(\theta + 1) \mp \frac{1}{3}\sqrt{\theta^2 - \theta + 1 + \frac{3}{A}\left(\frac{\alpha\beta}{\gamma} + 1\right)}$$

It is easy to check that for all $A >> 1$ and for sufficiently small α and β, we have

$$0 < e_1 < \theta < e_2 < 1.$$

Hence, the images of the two line segments

$$\{(e_1, u_2): \quad u_2 \in [r, s]\}, \quad \{(e_2, u_2): \quad u_2 \in [r, s]\}$$

lie outside of the rectagle $\mathbf{R}$. To complete the proof of Statement 1 we need to show that the three disjoint "horizontal" connected components of $f(\mathbf{R}) \cap \mathbf{R}$ do not overlap. it suffices to show that

$$f_2(u_1, u_2) \neq f_(u_1', u_2')$$

for distinct (u_1, u_2) and (u_1', u_2'). Indeed, $\beta u_1 + \gamma u_2 = \beta u_1' + \gamma u_2'$ implies $u_1 = u_1' + \frac{\gamma}{\beta}(u_2' - u_2)$. Since the map f is locally diffeomorphic in $f(\mathbf{R}) \cap \mathbf{R}$ we have that $|u_2' - u_2| > \varepsilon$. Hence, for sufficiently small β we obtain that $|u_1 - u_1'|$ becomes so large that the points u_1 and u_1' cannot both lie in $\mathbf{R}$. This completes the proof of Statement 1. The second statement follows from the first one.

We now establish the third statement. For each $p \in \mathbf{R}$ and $\lambda > 1$ define two cones

$$C^u(p) = \left\{ v = (v_1, v_2) \in T_p\mathbb{R}^2 : |v_2| \leq \lambda^{-1}|v_1| \right\},$$
$$C^s(p) = \left\{ v = (v_1, v_2) \in T_p\mathbb{R}^2 : |v_2| \geq \lambda|v_1| \right\}.$$

Note that $C^u(p)$ and $C^s(p)$ depend continuously on p, $C^u(p) \cap C^s(p) = \{p\}$, and the angle between $C^u(p)$ and $C^s(p)$ is a non-zero constant. For $v = (v_1, v_2) \in \mathbb{R}^2$ define $||v|| = ||(v_1, v_2)|| = \max(|v_1|, |v_2|)$.

Lemma 6.1.5. *There exists $\lambda > 1$ such that*

(a) *if $p \in \mathbf{R} \cap f^{-1}(\mathbf{R})$ and $v \in C^u(p)$ then $Df_p v \in C^u(f(p))$ and $||Df_p v|| \geq \lambda ||v||$;*

(b) *if $p \in \mathbf{R} \cap f(\mathbf{R})$ and $v \in C^s(p)$ then $Df_p^{-1}v \in C^s(f^{-1}(p))$ and $||Df_p^{-1}v|| \geq \lambda ||v||$.*

Proof of the Lemma. Let $p = (x, y)$, $f(p) \in \mathbf{R}$. For any $\gamma > 1$ one can define $C^{s,u}(p)$. Let $v = (v_1, v_2) \in C^u(p)$. Then we have $|v_1| \geq \lambda |v_2| > |v_2|$ and hence, $||(v_1, v_2)|| = |v_1|$. Set $(w_1, w_2) = Df_p(v_1, v_2)$. Let $\tilde{x}_1$ and $\tilde{x}_2$ be the roots of $h(x)$ defined in Lemma (6.1.4). For sufficiently large A we have that $f(\tilde{x}_2, y) > \ell$ and $f(\tilde{x}_1, y) < r$. Hence, if $(x, y), f(x, y) \in \mathbf{R}$ then $h(x) \neq 0$. For sufficiently large A we can choose $\lambda_1 > 1$ such that

(6.1.36) $$\frac{|1 + Ah(x)| - \alpha}{\beta + 1} > \lambda_1 > 1.$$

We have

$$|w_2| = |\beta v_1 + \gamma v_2| \leq \beta|v_1| + |v_2| \leq (\beta + 1)|v_1|$$

and

$$|w_1| = |(1 + Ah(x))v_1 - \alpha v_2| \geq |(1 + Ah(x))||v_1| - \alpha|v_2|$$
$$\geq |1 + Ah(x)||v_1| - \alpha|v_1| = (|1 + Ah(x)| - \alpha)|v_1|.$$

Hence,

$$|w_1| \geq \frac{|1 + Ah(x)| - \alpha}{\beta + 1}|w_2| \geq \lambda_1|w_2|.$$

for sufficiently large A. This implies that $(w_1, w_2) \in C^u(f(p))$ and

$$||(w_1, w_2)|| = |w_1| \geq (1 + \beta)\lambda_1|v_1| > \lambda_1|v_1| = \lambda_1||(v_1, v_2)||.$$

Statement (a) follows.

To prove Statement (b) let $p = (x, y)$, $f^{-1}(p) \in \mathbf{R}$ and $v = (v_1, v_2) \in C^s(p)$. Then $|v_1| \leq \lambda|v_2| < |v_2|$ and hence, $||v_1, v_2|| = |v_2|$. Let

$(w_1, w_2) = Df_p^{-1}(v_1, v_2)$. We have

$$Df_p^{-1} = \begin{pmatrix} \frac{\gamma}{m(x)} & \frac{\alpha}{m(x)} \\ -\frac{\beta}{m(x)} & \frac{1+Ah(x)}{m(x)} \end{pmatrix},$$

where $m(x) = \alpha\beta + \gamma(1 + Ah(x))$. It follows that

$$|w_1| = \frac{1}{|m(x)|}|\gamma v_1 + \alpha v_2| \le \frac{1}{|m(x)|}(\gamma|v_1| + \alpha|v_2|) \le \frac{\alpha + \gamma}{|m(x)|}|v_2|,$$

and

$$|w_2| = \frac{1}{|m(x)|}|(1 + Ah(x))v_2 - \beta v_1| \ge$$

$$\frac{1}{|m(x)|}|(1 + Ah(x))||v_2| - \beta|v_1| \ge \frac{|1 + Ah(x)| - \beta}{|m(x)|}|v_2|.$$

For sufficiently large A and sufficiently small α and β, one can choose $\lambda_2 > 1$ such that

$$\frac{|1 + Ah(x)| - \beta}{|m(x)|} > \lambda_2.$$

It follows that

$$|w_2| \ge \frac{|1 + Ah(x)| - \beta}{|m(x)|}|v_2| \ge \frac{|m(x)|}{\gamma + \alpha}\lambda_2|w_1| \ge \lambda_2|w_1|.$$

This implies that $(w_1, w_2) \in C^s(f^{-1}(p))$. It follows that

$$||(w_1, w_2)|| = |w_2| > \lambda_2|v_2| = \lambda_2||(v_1, v_2)||.$$

The desired result follows if we set $\lambda = \min\{\lambda_1, \lambda_2\}$.   □

It follows from the lemma that Λ is hyperbolic.

We now prove Statement 4 of the theorem. Clearly, $O \in \mathbf{R}$. It follows from (6.1.35) and (6.1.34) that

$$A > \frac{4(1 + 2\alpha s - \theta)}{(\theta + 1)(\theta - 1)^2} > \frac{4(1 + 2\frac{\alpha\beta}{1-\gamma} - \theta)}{(\theta + 1)(\theta - 1)^2} > \frac{4\alpha\beta}{(1 - \gamma)(1 - \theta)^2}.$$

Thus the condition (6.1.29) holds, and, hence, there are three fixed points, O and P_i, $i = 1, 2$. Finally, one has

$$\theta < x_1 < x_2 < 1, \quad \frac{\beta\theta}{1 - \gamma} < y_1 < y_2 < \frac{\beta}{1 - \gamma},$$

for x_i and y_i, $i = 1, 2$, defined by (6.1.28). It follows from (6.1.35) that

$$0 < y_1 < y_2 < s.$$

Hence, $P_1, P_2 \in \mathbf{R}$.   □
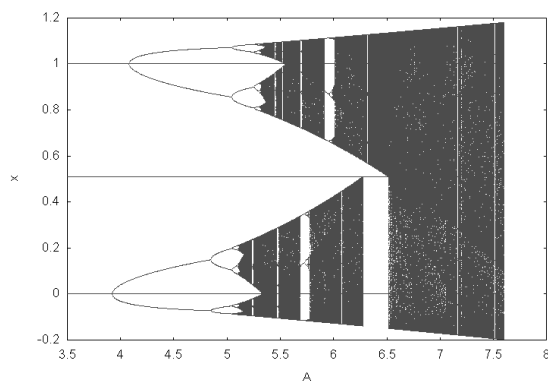
FIGURE 19. The bifurcarion diagram for the FitzHugh-Nagumo map, $\gamma = 0.1$, $\alpha = 0.01$, $\beta = 0.02$, $\theta = 0.51$.
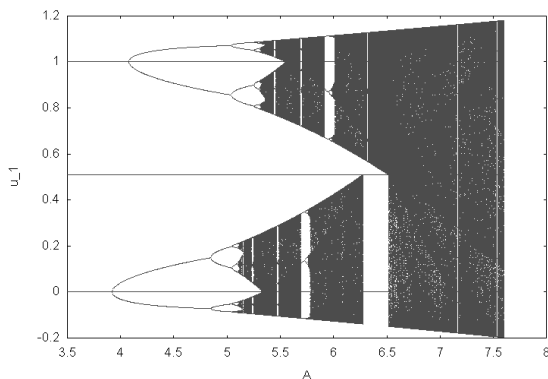

FIGURE 20. The bifurcarion diagram for the FitzHugh-Nagumo map, $\gamma = 0.52$, $\alpha = 0.01$, $\beta = 0.02$, $\theta = 0.51$.
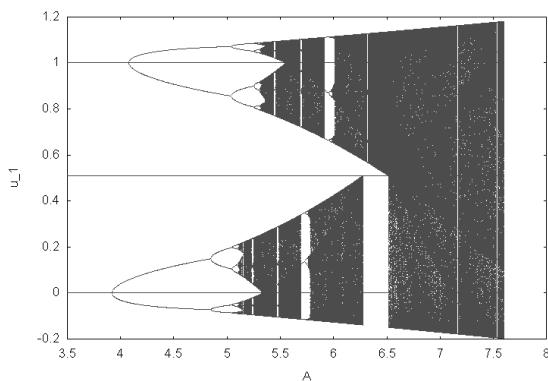

FIGURE 21. The bifurcarion diagram for the FitzHugh-Nagumo map, $\gamma = 0.9$, $\alpha = 0.01$, $\beta = 0.02$, $\theta = 0.51$.
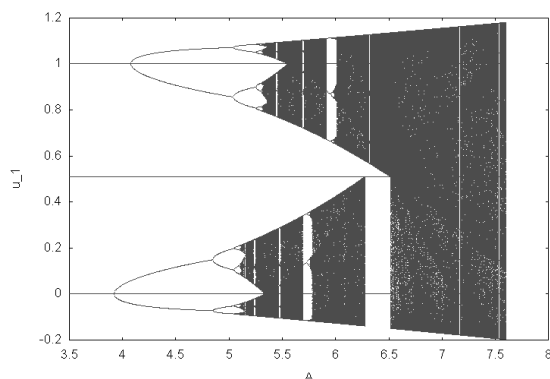
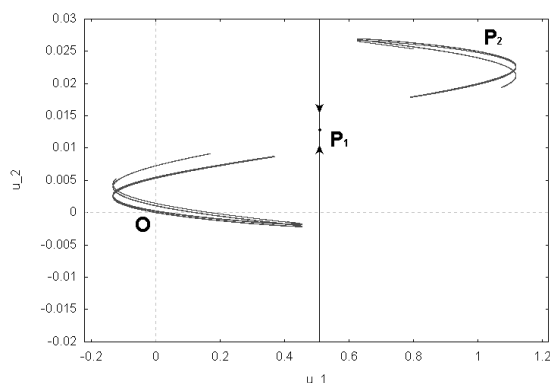FIGURE 22. The bifurcarion diagram for the Nagumo map, $\theta = 0.51$.

FIGURE 23. The attractor for the FitzHugh-Nagumo map, $\gamma = 0.2$, $\alpha = 0.01$, $\beta = 0.02$, $\theta = 0.51$, $A = 6.1$, $\mathbf{R} = [-0.21, 1.23] \times [-0.02, 0.031]$.

6.2. **Bifurcation Diagrams for the FitzHugh-Nagumo Equation.** In this section we give a computer-assisted analysis of the transition from the Morse-Smale type to the existence of the Hénon-like attractor as A increases.

Set $\alpha = 0.01$, $\beta = 0.02$, and $\theta = 0.51$ which satisfy the requirments of Theorems 6.1.1 - 6.1.3. Observe that the bifurcation diagrams appear to be identical for different values of γ (see Figure 19 - 21). Moreover, the bifurcation diagram for the FitzHugh-Nagumo equation (for the different values of γ) and the bifurcation diagram for the Nagumo equation (see 5.2) are also identical. In what follows we set $\gamma = 0.2$.

We have only one fixed point for $A < 4.1649313 \times 10^{-3}$ and three for $A > 4.1649313 \times 10^{-3}$ (see (6.1.27) and (6.1.29)).
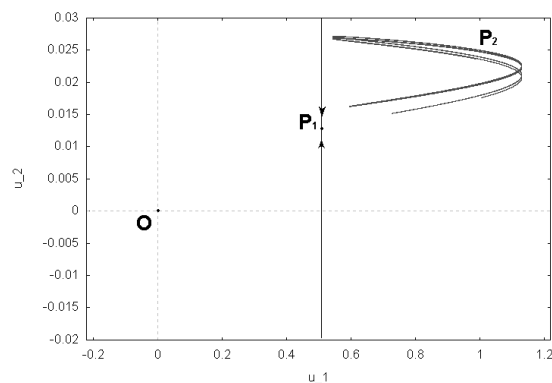
FIGURE 24. The attractor for the FitzHugh-Nagumo map, $\gamma = 0.2$, $\alpha = 0.01$, $\beta = 0.02$, $\theta = 0.51$, $A = 6.4$, $\mathbf{R} = [-0.21, 1.23] \times [-0.02, 0.031]$.
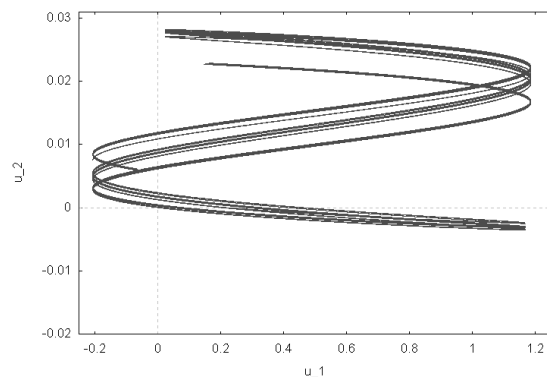

FIGURE 25. The attractor for the FitzHugh-Nagumo map, $\gamma = 0.2$, $\alpha = 0.01$, $\beta = 0.02$, $\theta = 0.51$, $A = 7.75$, $\mathbf{R} = [-0.21, 1.21] \times [-0.02, 0.031]$.

It follows from Theorem 6.1.1 that for small values of A the system is of Morse-Smale type. As A increases we observe two sequences of period doubling bifurcations around $A = 4$. The first sequence arises from O and the second one from P_2. It follows from Theorem 6.1.2 that for A between approximately 4 and 7.8 there is a trapping region (rectangle) $\mathbf{R}$, containing all three fixed points, and an attractor inside $\mathbf{R}$.

At first the attractor contains only finitely many attracting and hyperbolic periodic points and their unstable manifolds. As A increases the period doubling goes on and, as we believe, ends up with two Feigenbaum attractors (in general, these attractors appear for different values of A), one around P_2 and another one around O.

When A exceeds the value $A = 6$ two Hénon-like attractors appear around the same two fixed points, P_2 and O (they may correspond to different values of A). In each of these attractors the unstable manifold of the corresponding fixed point is dense The basins of attraction of these attractors are separated by the stable separatrix of the fixed point P_1 (see Figure 23).

For $A \approx 6.3$ the unstable separatrix of the fixed point O interesects the stable separatrix of P_1 and all orbits in $\mathbf{R}$ will go to the only Hénon-like attractor around P_2 (see Figure 24). This does not happen in the symetric case, $\theta = 0.5$.

As A increases even further (approximately above 6.5), the two attractors collide and the unstable separatrices of P_2 and O are dense in the resulting Hénon-like attractor (see Figure 25).

It follows from Theorem 6.1.3 that for large values of A the system has a horseshoe.

APPENDIX . PRELIMINARIES (SEE [15], [25], [23])

Consider a C^1 diffeomorphism $f : M \to M$ of a compact smooth Riemannian manifold M. We denote by $\Omega(f)$ the set of all nonwandering points and by $Per(f)$ the set of periodic points of f.

Recall that a diffeomorphism (endomorphism) f is called a *Morse-Smale diffeomorphism* (*endomorphism*) if

(1) $\Omega(f) = Per(f)$;
(2) every periodic point is hyperbolic;
(3) the global (local) stable and unstable manifolds of periodic points intersect transversally.

If a map $f : \mathbb{R}^d \to \mathbb{R}^d$ has ∞ as a fixed point (repelling or attracting), one can define the *compactification map* $\tilde{f} : S^d \to S^d$ by

$$\tilde{f} = P \circ f \circ P^{-1},$$

where $P : S^d \backslash \{N\} \to \mathbb{R}^d$ is the stereographic projection and N is the North Pole of S^d.

REFERENCES

[1] V. S. Afraimovich, Ya. Pesin, Travelling Waves in Lattice Models of Multi-dimensional and Multi-component Media: I. General Hyperbolic Properties, Nonlinearity, 6 (1993), 429-455.
[2] V. S. Afraimovich, Ya. Pesin, A. Tempelman, Travelling Waves in Lattice Models of Multidimensional and Multi-component Media: II. Ergodic Properties and Dimension, Chaos, 3 (1993), no. 2, 233-241.

[3] D. G. Aronson, H. F. Weinberger, Nonlinear Diffusion in Population Genetics, Combustion and Nerve Propagation, Lecture Notes in Mathematics, Springer-Verlag, vol. 446, 5-49 (1975).

[4] P. J. Blennerhassett, On the Generation of Waves by Wind, Philos. Trans. Roy. Soc. London Ser. A 298 (1980/81), no. 1441, 451-494.

[5] Bonhoeffer, Activation of Passive Iron as a Model for the Excitaion of Nerve, J. General Physiology, vol. 32 (1948), 69.

[6] J. Cronin, Mathematical Aspects of Hodgkin-Huxley Neural Theory, Cambridge UP (1987).

[7] M. C. Cross, P. C. Hohenberg, Pattern Formation Outside of Equilibrium, Reviews of Modern Physics, Vol. 65 (July 1993), No. 3, 851-113.

[8] I. R. Epstein, J. A. Pojman, An Introduction to Nonlinear Chemical Dynamics, Oxford UP (1998).

[9] R. A. Fisher, The Genetical Theory of Natural Selection, Oxford University Press (1930).

[10] R. A. Fisher, The Advance of Advantageous Genes, Annual of Eugenics, v.7 (1937), 355-369.

[11] R. FitzHugh, Impulses and Physiological Models of Nerve Membrane, Biophysical J., v.1 (1961), 445-466.

[12] R. FitzHugh, Biological Engineering, McGraw-Hill (1969), 1-85.

[13] A. V. Gaponov-Grekov, M. I. Rabinovich, Nonlinearities in Action, Springer-Verlag (1992).

[14] A. L . Hodgkin, A. F. Huxley, A Quantitative Description of Membrane Current and Its Application to Conduction and Excitation in Nerve, J. Physiology, v.117 (1952), 500-544.

[15] A. Katok, B. Hasselblatt, Introduction to the Modern Theory of Dynamical Systems, Cambridge University Press (1998).

[16] A. N. Kolmogorov, I. G. Petrovskii, N. S. Piskunov, A Study of the Diffusion Equation with Increase in the Amount of Substance, and Its Application to a Biological Problem in Selected Works of A. N. Kolmogorov, vol. 1, 242-270, Kluwer Academic Publishers (Appeared in Bull. Moscow Univ., Math. Mech. 1:6, 1-26, 1937).

[17] K. Maginu, Reaction-Diffusion Equation Describing Morphogenesis. I. Waveform Stability of Stationary Solutions in a One Dimensional Model, Mathematical Bioscience, vol. 27 (1975), 17-98.

[18] C. Marchioro, M. Pulvirenti, Mathematical Theory of Incompressible Nonviscous Fluids, Springer-Verlag (1994).

[19] N. Minorsky, Introduction to Non-linear Mechanics, J. W. Edwards (1947).

[20] J. D. Murray, Mathematical Biology, Springer (1993).

[21] J. Nagumo, S. Arimoto, S. Yoshizawa, An Active Pulse Transmission Line Simulating Nerve Axon, Proceedings of the IRE, October 1962, 2061-2070.

[22] J. Nagumo, S. Arimoto, S. Yoshizawa, Bistable Transmission Lines, IEEE Trans., Circuit Theory, 12 (1965), 400-412.

[23] Z. Nitecki, Differential Dynamics, The MIT Press (1971).

[24] D. R. Orendovici, Ya. B. Pesin, Chaos in Traveling Waves of Lattice Systems of Unbounded Media, Numerical methods for bifurcation problems and large-scale dynamical systems, 327-358, IMA Vol. Math. Appl., 119, Springer (2000).

[25] J. Palis, W. de Melo, Geometric Theory of Dynamical Systems, Springer-Verlag (1982).

[26] C. V. Pao, Nonlinear Parabolic and Elliptic Equations, Plenum Press (1992).

[27] C. Rocsoreany, A. Georgescu, N. Giurgiteanu, The FitzHugh-Nagumo Model, Kluwer Academic Publisher (2000).

[28] K. Stewartson, J. T. Stuart, A Non-linear Instability Theory for a Wave System in Plane Poiseuille flow, J. Fluid Mechanics, vol. 48 (1971), part 3, 529-545.

[29] A. M. Turing, The Chemical Basis of Morphogenesis, Phil. Trans. Roy. Soc. B, vol. 237 (1952), 5-72.

[30] F. Verhulst, Nonlinear Differential Equations and Dynamical Systems, Springer-Verlag, 1990.

DEPARTMENT OF MATHEMATICS, PENNSYLVANIA STATE UNIVERSITY, UNIVERSITY PARK, STATE COLLEGE, PA 16802
    E-mail address: pesin@math.psu.edu

SCHOOLOF MATHEMATICS, GEORGIA INSTITUTE OF TECHNOLOGY, ATLANTA, GA 30332
    E-mail address: yurchenk@math.gatech.edu